Citation: Shalaby, I., T. Hayashida (2023), Ground motion simulation of a significant earthquake in Egypt, Synopsis of IISEE-GRIPS Master's Thesis.

GROUND MOTION SIMULATION OF A SIGNIFICANT EARTHQUAKE IN EGYPT

Ibrahim SHALABY[1]
MEE22702

Supervisor: Takumi HAYASHIDA[2*]

ABSTRACT

Destructive and significant earthquakes like the 1992 Dahshur Earthquake (Mb 5.8) in Egypt, which caused extreme damage to lives and property, high mortality, and severe injuries, may happen again with similar or different magnitudes and intensities. Earthquake simulation requires three pieces of information: source effect, wave propagation path, and site amplification factors. This study aims to separate the source, site, and path effects of earthquakes recorded by the Egyptian Strong-Motion Network (ESMN) to simulate ground motions from a significant earthquake that may recur in Egypt. We applied the spectral inversion method (generalized spectral inversion technique; GIT) using the ground motion records observed at 20 stations for 52 earthquakes (M3–7.8) to separate the factors. We regarded station HLWN as a reference rock site and station ANSH as a divisor that recorded the maximum number of events. Finally, we simulated the ground motions for a potential earthquake in Cairo (Mw7.0), using the derived information from GIT and phase information from a small earthquake in Cairo. The simulated waveform indicates peak ground accelerations of 58 cm/s^2 at station HLWN, about 35 km from the epicenter, suggesting the possibility of widespread strong ground motions in populated areas. This study shows that GIT can provide physics-based ground motion estimations in Egypt.

Keywords: Spectral inversion, Site amplification, Attenuation factor, Reference site, ESMN.

1. INTRODUCTION

The earthquake-induced ground shaking (i.e., earthquake ground motion) is mainly controlled by the earthquake source, propagation path, and site amplification factors. While seismic source characteristics are related to the earthquake generation process associated with the fault rupture phenomenon, propagation characteristics are related to the wave propagation of the seismic waves emitted from the seismic source. Site characteristics, also known as ground motion amplification characteristics, indicate the effects of seismic wave amplification on shallow sediments. These characteristics contribute to ground-motion prediction in a complex manner. Accordingly, science and engineering research is being actively pursued. Many research findings were based on exhaustive surveys of damaged areas. In Egypt, two earthquakes (in southwest Cairo on 12 October 1992, and Gulf of Aqaba on 22 November 1995) caused damage in populated areas. During the 1992 Cairo earthquake, the most severely affected regions were Old Cairo, Bulaq, and areas extending southwards along the Nile. This event resulted in the destruction of 350 buildings and extensive damage to 9,000 others. Additionally, 216 mosques and 350

[1] National Research Institute of Astronomy and Geophysics (NRIAG)-Helwan-Cairo-Egypt.
[2] International Institute of Seismology and Earthquake Engineering, Building Research Institute.
* Chief examiner

schools suffered significant harm, leading to approximately 30,000 families being displaced from their homes.

The generalized spectral inversion technique (GIT) is employed to identify the spectral shapes of the strong motions dividing earthquake records into the source, propagation path, and site amplification factors. This method assists in deducing the physical factors that govern the mechanisms considered in ground motion generation, and it facilitates the creation of accurate models by utilizing information from the Fourier amplitude spectra (FAS). This study determined the strong ground motion parameters observed by the Egyptian Strong Motion Network. We also attempted to estimate ground motions at current seismic stations for a possible earthquake with a magnitude of Mw7.0.

2. DATA

In this work, 52 strong-motion earthquakes were gathered from 20 stations containing 206 acceleration records. The magnitude ranged from 3 to 7.8. The events were recorded from 2008 (when the ESMN was constructed) to 2023. The acceleration waveforms were recorded in unit m/s^2 or count. The file formats were seed, mseed, and ASCII, all converted to the sac format. This dataset was manually selected from approximately 8000 local and regional earthquakes that happened in Egypt and around Egypt, and that were recorded in the NRIAG bulletin and the GCMT catalog using the Compass 2014 software and by applying a band-pass filter to clear the events recorded in our stations. The file format was converted to the SAC format using the same software. To convert the data from count to gal, we use the formulas shown in Table 1. for each sensor.

Table 1. Conversion coefficients from count to gal (cm/s^2).

Type of sensors	The equation used
Reftek	$(0.66\times10^{-6}) \times$ (readings)
Titan	$(0.0625\times10^{-6}) \times$ (readings)
Kinemetrics	$(0.119\times10^{-6}) \times$ (readings)
Guralp	$(0.981\times10^{-6}) \times$ (readings)

Two or three different sensor types were changed at the same station during the measurement period, or the same sensor was replaced at a different station in a different period. All the record names at the same station were renamed in this work, even with different sensor types, to only one name for each station.

3. METHODOLOGY

3.1. Earthquake parameters separation

The GIT is based on a mathematics concept, in which the Fourier amplitude spectra of the ground motion are expressed in the frequency domain as the product of three factors; $S_i(f)$ the spectrum of the source associated with the *i*th earthquake, $P_{ij}(f, X_{ij})$ is the function of distance and frequency accounting for the path effects and $Gj\ (f)$ is the site response function of the *j*th station as expressed in Eq. (1):

$$F_{ij}(f, X_{ij}) = S_i(f) \cdot P_{ij}(f, X_{ij}) \cdot G_j(f) \quad (1)$$

The term $P_{ij}(f, X_{ij})$ by Boore (1983) was presented as a function of S-wave velocity along the path V_s, the frequency-dependent quality factor $Q(f)$ and hypocenter distance X_{ij} as follows:

$$P_{ij}(f, X_{ij}) = \frac{1}{X_{ij}} exp\left(\frac{-\pi f X_{ij}}{V_s Q(f)}\right) \quad (2)$$

The following is obtained when substituting Eq. (2) in Eq. (1):

$$F_{ij}(f, X_{ij}) = S_i(f) \,.\, G_j(f) \,.\; X_{ij}^{-1}\, exp\left(\frac{-\pi f X_{ij}}{V_s Q(f)}\right) \tag{3}$$

The parameters are separated by taking the natural logarithm of the left and right sides. We applied for four Fortran programs following Iwata & Irikura (1988), developed by Dr. Hayashida (IISEE-BRI). Only S-wave was used for the treatment; hence, the first program extracted the S-wave part, in which the first 10.24 s from the S-wave onsets. Fast Fourier transform (FFT) was also performed for the selected data to obtain the Fourier spectra and horizontal-to-vertical (H/V) spectral ratios of the extracted waves. The second program was implemented to create the matrices using the accepted dataset. The third program stabilizes the inversion problem by choosing some known parameters. From H/V results, we assumed station HLWN as a reference rock site, assuming the amplification factor as $G_j(f) = 2$, and station ANSH as a divisor site. The final program derives the estimated source, site amplification, and attenuation path factor by conducting a linear inversion analysis.

3.2. Simulation of potential earthquake

This study mainly aimed to simulate an earthquake in Egypt that may recur at the source, similar to that of the historically significant and destructive earthquakes in Egypt. The most recent major earthquake is the 1995 Gulf of Aqaba earthquake (Mw7.3), but the small earthquake ground motion records that occurred near the epicenter, which are necessary to reproduce it, are not included in our data set. On the other hand, we assumed a Mw7.0 earthquake in Cairo for the simulation.

Earthquake simulation requires the recorded data of a smaller earthquake (i.e., target earthquake) at the same location. We did not have a record of the 1992 earthquake, but we have the data from three stations for the 202012111547 event. By comparison, this event was the closest to the 1992 Dahshur Earthquake, bearing only a small location difference. Hence, it was considered herein as a target earthquake.

The following parameters to simulate the waveforms should be estimated: Fourier amplitude spectra for the target large earthquake and phase spectra from the small earthquake. Three parameters were needed to model the amplitude spectra, namely, the source, path (Q factor), and site effects. For the source effect, we had the pseudo-point source models (Nozu, 2012) that followed the assumption of an omega square model based on the earthquake source model proposed by Brune (1970). The flat level (Ω_o) and the corner frequency (f_o) were estimated from the seismic moment (M_o) to define the source spectrum of the simulated event. The formula of Hanks and Kanamori (1979) was used to calculate the seismic moment (M_o) from moment magnitude M_w, from Eq. (4) we assumed (M_w=7) we found M_o = 3.55e + 26 dyne.cm. where:

$$M_o = 10^{1.5\,(M_w + 10.7\,)} \tag{4}$$

The corner frequency (f_o) was estimated by following the empirical formula of Kawase & Matsuo (2004) Eq. (5) by substitute with M_o, we found $f_0 = 0.035$ Hz.

$$M_o = 8.0 \times 10^{22} \times {f_0}^{-2.5015} \tag{5}$$

All these parameters were employed to determine the source effect for the potential earthquake follow formula of David & Boore, (1983):

$$S\,(f) = R\theta\phi \,.\, fs \,.\, PRTITN \,.\; \frac{M_0}{4\pi\rho\beta^3} \;.\; \frac{(2\pi f)^2}{1+(\frac{f}{f_0})^2} \tag{6}$$

where, $S(f)$ is Fourier amplitude spectra, $R\theta\phi$ = 0.55 is the radiation pattern, fs = 2 is the free surface effect, $PRTITN$ = $\frac{1}{\sqrt{2}}$ is coefficient that separate the horizontal motion into two component, ρ=2.4 g/cm^3 is the density and β=3.55 km/s is the S-wave velocity.

Now we have the phase of the simulated earthquake where it is the same as the target earthquake. From Eq. (6), we obtained the source spectrum of the target earthquake, and we considered the estimated site effect and Q-factor to model the amplitude spectra at the given site. Our target stations are HLWN, KOTM, and DABA.

By compiling the Fourier amplitude spectra and the corresponding phase of the potential earthquake with magnitude Mw7.0 at the location of the 1992 Dahshur Earthquake. The spectra were converted to the time domain at the station that recorded the target earthquake.

4. RESULTS AND DISCUSSION

4.1. Earthquake parameters separation

By applying the four Fortran programs with some characteristic and changing the characteristics and trying again, the programs exclude some data, finally we get the suitable results by using 137 records at 15 stations from 19 events. As clear in Figure 1. The estimated site amplification factors assuming the HLWN station as a reference site. We plotted the amplification spectra in the frequency range of 0.2 to 10 Hz for each station. Almost all the station site amplifications decreased when the frequency increased. This was mainly observed in frequencies higher than 1.0 Hz. In addition, some stations presented strange site effect values higher than 10, which may be attributed to the data rarity and sensor history in these sites, where each sensor had a different conversion equation from count to gal (cm/s^2), as shown in Table 1. Also, the results show that at some sites the amplification factor estimated is similar to the H/V spectral ratio.

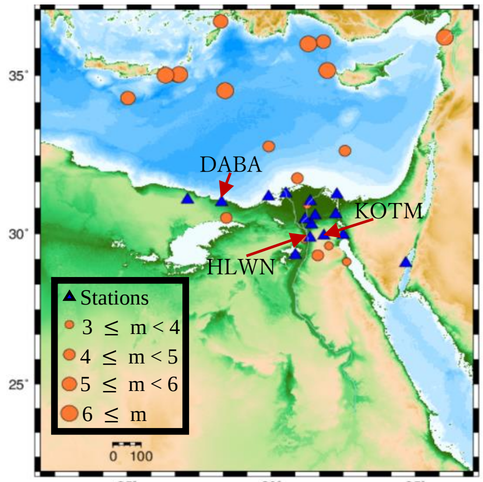

Figure 1. Epicenters of the events used in this study (circles) and the ESMN stations (triangles).

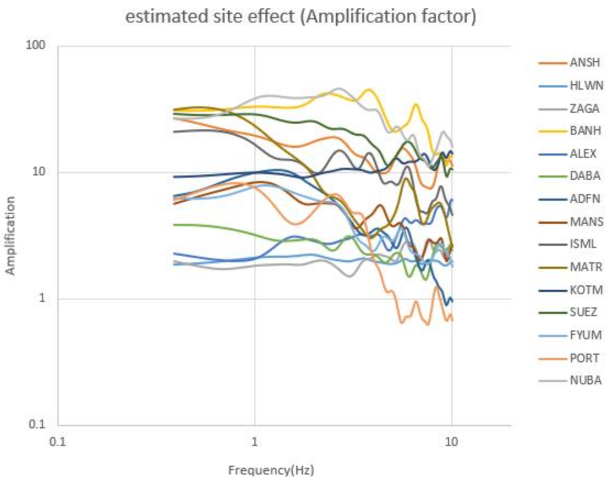

Figure 2. Estimated site amplification factors at each frequency at each station.

The estimated Q factors are plotted in Figure 3 in the frequency range of 0.2 to 10 Hz. The attenuation model (Q factor) is derived as a function of the frequency Q(f) = B f^{α} using the least square method. Accordingly, B = 186.86 and α = 1.5 are obtained. The estimated Q factors show frequency dependency.

Concerning source factors, we plot the estimated source factors as a function of the frequency from 0.2 to 10 Hz for all events accepted in the inversion using the reference site constraint. The source spectral decay shows that all estimated source spectra for all events rapidly decrease at a frequency greater than 1 Hz. The source spectra illustrate frequency dependence. We did not examine the seismic moment (M_0), where the frequency band is limited, as shown in Figure 4.

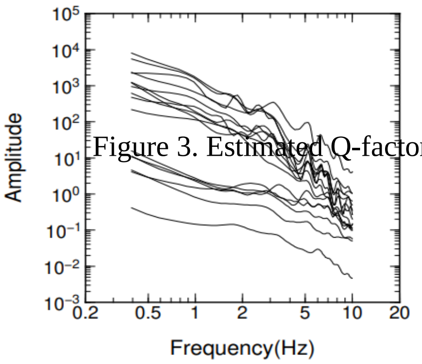

Figure 4. Estimated source factors for all accepted events.

4.2. Simulation of potential earthquake

The simulated and target earthquakes were approximately at the same location, 35 km from HLWN station, 78 km from KOTM station and 320 km from DABA station. The peak ground amplitudes (PGA) at station DABA show small values; 1.7 gal and 2.2 gal in N-S and E-W components, respectively. Station KOTM is located farther than station HLWN from the epicenter, but the estimated PGAs are 65 gal and 70 gal in N-S and E-W component, respectively. The PGAs at station HLWN, the PGA values are 58 gal and 50.4 gal in N-S and E-W component, respectively, implying that station KOTM is located on soft sediment.

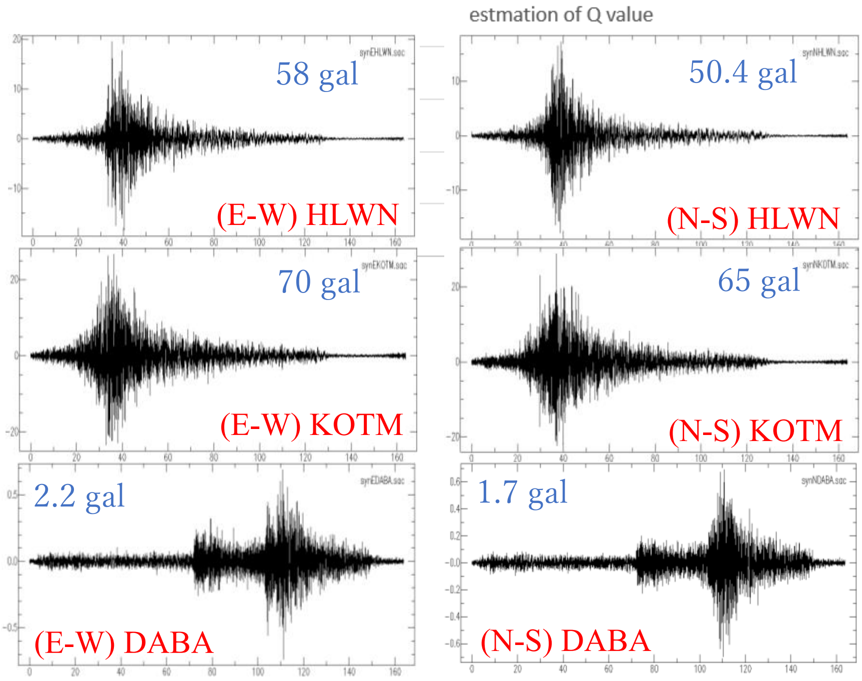

Figure 5. Simulated waveform and PGA values for an M7 earthquake (Mw7.0) at the E–W and N–S components of the HLWN, KOTM and DABA stations (see location in Figure 1).

5. CONCLUSIONS

This study focused on separating the source, path, and site effects from the recorded strong-motion data in the ESMN from 2013 to 2023. The spectral inversion method was applied to separate the three factors of source, path, and site. It used the S-wave portion of the observed acceleration Fourier spectra to estimate the site amplification and the Q factor in the 0.2 to 10 Hz frequency range.

The HLWN station was chosen as a reference rock site, to stabilize the inversion, considering the S-wave H/V ratio information. The estimated amplification factor in the HLWN station also confirmed its ability to be a reference site.

Estimating the source factors resulted in the 0.2 to 10 Hz frequency range for all the events used in the inversion, which employed the reference site constraint. The source spectral decay showed that all estimated source spectra for all events rapidly decreased at a frequency greater than 1 Hz. The source spectra displayed frequency dependence. The Q factor was calculated where the $Q(f) = 186.86\ f^{1.5}$, which clearly showed frequency independent.

Finally, we simulated ground motions waveforms for the potential earthquake in Cairo (M_w=7.0). The Fourier amplitude spectra at the three sites target were obtained from the site, path, and source effect parameters for the potential earthquake. The Fourier phase spectra were obtained from the small earthquake recordings at the same location. The estimated waveforms show that PGAs at station KOTM are larger than station HLWN located closer to the epicenter, implying a larger site amplification. Our estimates suggest that the ground motions around Cairo will be large for the potential earthquake due to subsurface soils, indicating the importance of evaluating ground motions at many sites, considering the detailed source model and site amplification factors.

ACKNOWLEDGEMENTS

This research was conducted during the individual study period of the training course "Seismology, Earthquake Engineering and Tsunami Disaster Mitigation" by the Building Research Institute, JICA, and GRIPS. I would like to thank all professors and the administration staff of these entities. Also, I would like to express my sincere gratitude to my supervisor Dr. Takumi Hayashida for his valuable support and experience which helped me to complete my research successfully. And thank my institute professors and colleagues who provide me with data.

REFERENCES

Boore, D. M. (1983). Stochastic simulation of high-frequency ground motions based on seismological models of the radiated spectra. *Bulletin of the Seismological Society of America*, *73*(6A), 1865-1894.

Brune, J. N. (1970). Tectonic stress and the spectra of seismic shear waves from earthquakes. *Journal of geophysical research*, *75*(26), 4997-5009.

Hanks, T. C., & Kanamori, H. (1979). A moment magnitude scale. *Journal of Geophysical Research: Solid Earth*, *84*(B5), 2348-2350.

Iwata, T., & IRIKURA, K. (1988). Source parameters of the 1983 Japan Sea earthquake sequence. *Journal of Physics of the Earth*, *36*(4), 155-184.

KAWASE, H., & MATSUO, H. (2004). Separation of source, path, and site effects based on the observed data by K-NET, KiK-net, and JMA strong motion network. *Journal of Japan Association for Earthquake Engineering*, *4*(1), 33-52.

Moya, A., & Irikura, K. (2003). Estimation of site effects and Q factor using a reference event. *Bulletin of the Seismological Society of America*, *93*(4), 1730-1745.

Nozu, A. (2012). A simplified source model to explain strong ground motions from a huge subduction earthquake-simulation of strong ground motions for the 2011 off the Pacific Coast of Tohoku Earthquake with a pseudo point-source model. *Journal of the Seismological Society of Japan, 65, 45-67.*